

Behavior of Prestressed Concrete Beam using Reactive Powder Concrete

Ignatius H. Sumartono^{a*}, Heru Purnomo^b, Sidiq Purnomo^c, Feryandy Murdono^c

Correspondence

^aMaster student in the Civil Engineering Department, University of Indonesia, UI Campus, Depok, Jawa Barat 16044, Indonesia.

^bProfessor in the Civil Engineering Department, University of Indonesia, UI Campus, Depok, Jawa Barat 16044, Indonesia.

^cResearcher in PT Wijaya Karya Beton Tbk., Jakarta 16044, Indonesia.

Corresponding author email address:
ignatiusharrysumartono@gmail.com

Submitted : 05 September 2023

Revised : 03 October 2023

Accepted : 21 October 2023

Abstract

The behavior of prestress pretension beams made of Reactive Powder Concrete (RPC) concrete with compressive strength above 120 MPa included in the Ultra High Performance Concrete (UHPC) classification was investigated to study the mechanical properties of concrete and the performance of prestressed beams against static load tests. The mechanical properties of RPC materials include concrete compressive strength, concrete tensile strength, concrete elastic modulus values and concrete density compared to 70 MPa High Strength Concrete (HSC) concrete. Curing concrete at an early age using high temperature hot steam (steam curing) ensures the development of the compressive strength of concrete. Experimental tests were carried out on 4 pretension beams designed to be used as highway bridge beams, namely beam #1 (30/50-HSC-NF-S); beam #2 (30/50-RPC-F-S); beam #3 (17/50-RPC-NF-S); beam #4 (17/50-RPC-NF-S). The mechanical properties of RPC concrete show superior values compared to HSC concrete. From the results of the static test, only beam #3 (RPC beam which does not use steel fiber in mixing) which shows a value of flexural resistance below the theoretical value due to brittle destruction that occurs in the beam. Steel fiber effectively maintains beam integrity thereby maximizing bending resistance, preventing explosive brittle destruction, and preventing concrete fragmentation during peak loads.

Keywords

Reactive powder concrete, ultra high performance concrete, high strength concrete, steel fiber, prestension beam

INTRODUCTION

Utilization of Reactive Powder Concrete (RPC) material as a structural component in Indonesia is still limited to material research and has not been implemented on a construction scale. The main factor that challenges the application of RPC on an industrial scale is the high construction costs for making RPC, on the other hand the low intensity of RPC material research to the research stage that is reliable for implementation as a structure makes the level of reliability of this RPC material often doubted when proposed for structural components. building. Reactive Powder Concrete is included in the Ultra-High Performance Concrete (UHPC) group which is defined from its compressive strength characteristics as a concrete group with a concrete compressive strength above 150 MPa. However, this grouping is not used universally. Canada Standard Association (CSA) classifies RPC in 2 classes based on compressive strength, namely compressive strength above 120 MPa and above 150 MPa [1]. RPC has very good performance where the concrete material properties are more ductile and have better durability compared to normal concrete [2]. The ductile nature of RPC is obtained from steel fiber which provides a bridging effect so that the failure mode is ductile and the material does not experience fragmentation [3], but steel fiber contributes significantly to the high production costs.

The studies that have been conducted on UHPC/RPC materials in Indonesia are still low, Nurjannah researched RPC for use as a beam-column subbasement in buildings [4], Hardjasaputra researched fire resistance for RPC in infrastructure buildings with fiber variations [5]. Both studies were conducted using Polyvinyl Alcohol Fiber (PVA fiber), and did not use steel fiber. Steel fiber has been produced and widely used in Indonesia, but currently the available steel fiber specifications are limited to a tensile strength of 1345 MPa. The reference used from research that has been carried out abroad uses steel fiber with a tensile strength of up to 2400 MPa, but the steel fiber available in Indonesia has never been investigated that it can be used to reduce the cost of making RPC.

The very high compressive strength of RPC concrete has the potential to be used as beams in bridge structures, but research on RPC using local materials in Indonesia as bridge beams has never been carried out. In this paper, the authors investigate prestressed RPC beams with a pretensioned system using RPC made from materials available in Indonesia. In this study, testing of concrete specimens was carried out to determine the physical and mechanical properties of RPC concrete and static load test experiments on prestressed RPC beams at a scale of 1: 1 which aimed to investigate the performance of the prestressed. The value of the beam flexural strength test results obtained from the experiment was then compared with theoretical calculations.

RESEARCH SIGNIFICANCE

This study aims to investigate the behavior of concrete materials and prestress pretension beams made by Reactive Powder Concrete (RPC) materials and also to determine concrete parameters to be used when designing structural components, investigate flexural resistance of prestress pretension beams with dimensional variations due to static loads designed as highway bridge beam components and knowing the potential problems when making RPC concrete on a mass industrial scale. This research is expected to contribute to supporting the world of construction in Indonesia to maximize the utilization of advanced concrete technology which has performance that is much more reliable than currently used, especially for implementation on precast prestress beams which are commonly used in bridge structures.

METHODOLOGY

The research method starts from literature studies of various journals and books from various sources, planning of concrete test specimens and prestressed beam specimens, experimental activities to obtain a result which is then analyzed and compared to theoretical results.

A. LITERATURE REVIEW

The idea of making Reactive Powder Concrete (RPC) is to increase the "Packing Density" of the cement matrix by reducing the extreme value of the water to cement ratio, replacing macro-sized coarse and fine aggregates with fine aggregates in the nanometer size range [5]. Optimal microstructure results from the accuracy of particle size gradations so as to produce maximum density. To achieve homogeneity of the concrete, the coarse gravel aggregate was replaced with fine sand with a maximum size of 250 μm , quartz sand with an average size of 10 μm . Silica fume is used to reduce the ratio of water to cement and increase the workability of the concrete mix to produce the highest hydration strength and high durability. Steel fiber is used to increase the ductility of concrete and the compactness of the material. The materials for making RPC concrete can be seen in Figure 1.



Figure 1 RPC concrete materials

The RPC mixture uses more silica fume which is very small in size and has pozzolanic properties, and uses a high amount of Portland cement to produce optimal compressive strength from the hydration process [6]. Silica fume is an amorphous material so it can react in the cement

hydration process. the content of Silicon Dioxide (SiO_2) in silica fume is reactive to Calcium Hydroxide ($\text{Ca}(\text{OH})_2$) resulting from the cement hydration process thereby increasing the speed of hydration of C_3S in the cement to become Calcium Silicate Hydrate ($\text{C}_3\text{S}_2\text{H}_3$ and CH) which strengthens the bond between cement particles and increase the strength of the concrete mixture in the first two days of concrete life [7]. This reaction can be active at high temperature conditions, therefore during the initial age it is necessary to treat concrete using high temperature hot steam (Steam Curing) to ensure the development of concrete compressive strength [8]. Steam curing treatment does not damage the matrix of concrete formation because it avoids the reaction between alkali and silica and avoids the onset of delayed entry because the mortar does not use coarse aggregate [9].

RPC has good durability, suitable for structure that are exposed to aggressive environmental conditions due to the dense micro-structure of concrete which prevents the penetration of corrosive materials into the concrete. Further research has shown that RPC is also self-healing in which the observation of micro cracks shows that the micro cracks are closed again. Cement particles in concrete that are not completely hydrated due to the use of a small amount of water in the mixture (W/C ratio of about 0.2) increase the durability because the cement in the concrete can continue the hydration process if micro-cracks appear under the appropriate humidity conditions [2]. Steel fiber makes a good ductility response to RPC compared to concrete without steel fiber which immediately crumbles when it reaches its peak load [10]. The use of steel fiber provides a bridging effect on concrete so that the failure mode is ductile and the material does not experience fragmentation [3]. The optimum volume of the amount of steel fiber used is in the range of 2% - 3% of the concrete volume. The use of steel fiber can produce higher compressive strength and a significant addition of flexural strength compared to concrete that does not use steel fiber [10].

Seeing the advantages of compressive strength, RPC is suitable to be combined with prestress systems such as on bridge beams. The RPC can reduce beam dimensions and reduce the amount of reinforcement [9]. With a narrower cross-section of the beam, the weight of the superstructure is lighter so that the design for the column structure and bridge foundation can be more economical. From a commercial aspect, the RPC concrete using locally available materials can significantly reduce the cost of making RPC [10].

B. PRESTRESSED BEAM STRENGTH DESIGN

The flexural strength of prestressed concrete beam is calculated using the limit strength method as used in reinforced concrete design. In calculating this flexural strength, the stress of the prestressed steel is not using the yield stress (f_y) but using the prestressing steel stress when the nominal cross-sectional strength (f_{ps}) is reached. The f_{ps} value is calculated by the strain compatibility method as shown in Figure 2. As an alternative, if the effective stress in the prestressed reinforcement after losses (f_{pe}) is greater than 50% of the ultimate tensile stress prestressing steel (f_{pu}), then for members with fully attached tendons

(pretension system) stress of prestressing steel (f_{ps}), calculated by equation 1.

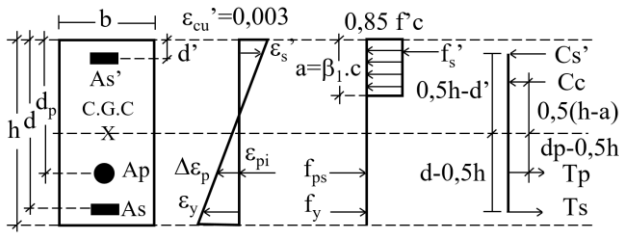


Figure 2 Square beam equivalent stress block

$$f_{ps} = f_{pu} \left\{ 1 - \frac{\gamma_p}{\beta_1} \left[\rho_p \frac{f_{pu}}{f_{py}} + \frac{d}{d_p} (w - w') \right] \right\} \quad (1)$$

If the compression reinforcement is taken into account, then the term:

$$\left[\rho_p \frac{f_{pu}}{f_{py}} + \frac{d}{d_p} (w - w') \right] \quad (2)$$

Equation 2 Values must be taken not less than 0.17 and $d \leq 0.15 d_p$

where:

- $\gamma_p = 0.55$ for $f_{py} / f_{pu} \geq 0.8$
- $= 0.40$ for $f_{py} / f_{pu} \geq 0.85$ (stress-relieved strand)
- $= 0.28$ for $f_{py} / f_{pu} \geq 0.90$ (low-relaxation strand)
- $\beta_1 = 0.85$ for $f'_c \leq 30$ MPa
- $= 0.85 - (f'_c - 30) * 0.008 \geq 0.65$ untuk $f'_c > 30$ MPa
- ρ_p = prestressed reinforcement ratio
- $= A_{ps} / (b * d_p)$
- ρ = non-prestressed tensile reinforcement ratio
- $= A_s / (b * d)$
- ρ' = compression reinforcement ratio
- $= A_{s'} / (b * d)$
- w = index of non-prestressed tensile reinforcement
- $= \rho (f_y / f'_c)$
- w' = compression reinforcement index
- $= \rho' (f_y / f'_c)$
- A_{ps} = area of prestressed reinforcement
- A_s = area of non-prestressed tensile reinforcement
- $A_{s'}$ = compression reinforcement area
- f'_c = compressive strength of concrete aged 28 days
- b = beam width
- d' = distance of the farthest compression fiber to the centroid of the compression reinforcement
- d_p = distance of the farthest compression fiber to the centroid of the prestressed steel
- d = distance of the farthest compression fiber to the centroid of the non-prestressed tensile reinforcement

To guarantee yielding of the reinforcement, the code limit¹, the value of the index of reinforcement for components² with prestressed reinforcement (ω_p), only as in equation 3.

$$\omega_p = \rho_p (f_{ps} / f'_c) \leq 0.36 \beta_1 \quad (3)$$

For members with prestressed and with tensile and compressive reinforcement, the limit index reinforcement as in equation 4.

$$\omega_p + (\omega - \omega') \frac{d}{d_p} \leq 0.36 \beta_1 \quad (4)$$

For the reinforcement index ratio that does not exceed the limit, the flexural strength is calculated by equation 5.

$$\phi M_n = \phi \left\{ C_c \left(\frac{h}{2} - \frac{a}{2} \right) + C_s \left(\frac{h}{2} - d \right) + T_s \left(d - \frac{h}{2} \right) + \left(d_p - \frac{h}{2} \right) \right\} \quad (5)$$

where:

- ϕ = flexural reduction factor
- h = beam height
- a = compressive block height of strain compatibility
- C'_c = concrete block compression force
- $= 0.85 f'_c * b * a$
- C'_s = compression reinforcement force
- $= A_{s'} * f'_s = A_{s'} * \epsilon'_s * E_s$
- T_s = non-prestressed reinforcement tension force
- $= A_s * f_y$
- T_p = prestress reinforcement tension force
- $= A_{ps} * f_{ps}$

Beams exhibit ductile behavior if they have sufficient postcracking capacity and yield tensile reinforcement before the concrete crumbles. To ensure that the beam has sufficient post-cracking capacity, the beam must have a strength reserve after cracking by fulfilling equation 6.

$$\phi M_n \geq 1.2 M_{cr} \quad (6)$$

where:

- ϕM_n = flexural moment capacity of the beam,
- M_{cr} = moment capacity that causes the beam stress to reach the modulus of rupture (f_r).

For beam sections with prestressed steel tendons, the beam cracking moment (M_{cr}), is calculated by equation 6.

$$M_{cr} = S_c * \left(-\frac{P_{eff}}{A_c} - \frac{P_{eff} f * e}{S_c} - f_r \right) \phi M_n \geq 1.2 M_{cr} \quad (7)$$

where:

- S_c = section modulus of the beam section
- A_c = beam cross-sectional area
- P_{eff} = effective prestressing force at the cross-section of the beam
- e = eccentricity of the center of gravity of the prestressing steel with the center of gravity of the beam section
- f_r = concrete modulus of rupture

The effective prestressing force acting is the prestressing force at the time of transfer which has been reduced by the loss of prestressing force calculated using equation 7.

$$P_{eff} = (f_{pi} - \Delta f_{PT}) * A_{ps} \quad (8)$$

where:

f_{pi} = prestressing steel stress at transfer
 Δf_{PT} = total loss of force in prestressing steel
 A_{ps} = area of prestressed reinforcement

$$\varepsilon_{CR} = C_t \frac{f_{cs}}{E_c} \quad (14)$$

For pretensioned beams system, the total loss of prestressing force (losses) is calculated by equation 9.

$$\Delta f_{PT} = \Delta f_{PES} + \Delta f_{PR} + \Delta f_{PCR} + \Delta f_{PSH} \quad (9)$$

where:

Δf_{PES} = loss due to elastic shortening of concrete
 Δf_{PR} = loss due to relaxation of the prestressing steel
 Δf_{PCR} = loss of force due to the effect of creep
 Δf_{PSH} = loss of force due to shrinkage

After stress transfer, the beam shortens which causes loss of prestressing force. Loss of prestress due to concrete elastic shortening is calculated by equation 10.

$$\Delta f_{PES} = \frac{E_{ps}}{E_{ci}} f_{cs} \quad (10)$$

where:

f_{cs} = concrete stress at the tendon level due to the initial prestressing force
 E_{PS} = modulus elasticity of prestressing steel
 E_{ci} = modulus elasticity of concrete during prestress transfer

If the center of gravity of the prestressed steel tendons has an eccentricity (e) with respect to the center of gravity of the cross-section of the beam and the moment due to self-weight (M_D) is taken into account, then f_{cs} is calculated by equation 11.

$$f_{cs} = -\frac{P_i}{A_c} - \frac{P_i * e^2}{I_c} + \frac{M_D * e}{I_c} \quad (11)$$

where:

P_i = prestressing force on transfer
 A_c = beam cross-sectional area
 I_c = beam cross sectional inertia

Loss of prestressing force due to relaxation of prestressed steel is calculated by equation 12.

$$\Delta f_{PR} = f_{pi} \frac{\log t}{45} \left(\frac{f_{pi}}{f_{py}} - 0,55 \right) \quad (12)$$

where:

f_{pi} = prestressing steel stress at transfer
 f_{py} = yield stress of pre-stressed steel
 t = time (in day)

Loss of prestress due to concrete creep is calculated by equation 13.

$$\Delta f_{PCR} = \varepsilon_{CR} * E_{PS} \quad (13)$$

where:

ε_{CR} = concrete creep strain
 E_{PS} = modulus elasticity of prestressing steel

The creep strain value of concrete, ε_{CR} , is calculated using equation 14.

where:

C_t = creep constant
 E_c = modulus elasticity of concrete
 f_{cs} = concrete stress at the tendon level due to the initial prestressing force

The creep constant (C_t) is calculated by equation 15 under the condition that the loss of prestressing force is assumed to be stable at 5 years.

$$C_t = \frac{t^{0,6}}{10 + t^{0,6}} C_u \quad (15)$$

where:

C_u = ultimate creep (can be taken value 2.35)
 t = time (in day)

Loss of prestress due to concrete shrinkage is calculated by equation 16.

$$\Delta f_{PSH} = \varepsilon_{SH} * E_{PS} \quad (16)$$

where:

ε_{SH} = concrete shrinkage strain
 E_{PS} = modulus elasticity of prestressing steel

The shrinkage strain that occurs in concrete for curing concrete with the steam curing method can be calculated by equation 17.

$$\varepsilon_{SH} = \frac{t}{55 + t} (\varepsilon_{SH})_u \quad (17)$$

where:

$(\varepsilon_{SH})_u$ = ultimate shrinkage strain (820x10-6 mm/mm)
 t = the time (in days) after the start shrinkage is reviewed

C. MAKING OF TEST SPECIMENTS

Test experiments are planned to investigate the physical and mechanical properties of RPC concrete and static loading behavior on pretension RPC beams. The specification of test specimens for beams are shown in Figure 3. Beam specifications were obtained from the calculation of prestressed beams for bridges with loads referring to SNI for bridge loading [11] and SNI for concrete structure planning for bridges [12]. The span of the bridge used is 7 m and the distance between the beams is 185 cm. The beam will behave compositely with a concrete slab as a vehicle floor with a thickness of 20 cm made at the bridge site. Identification of beam specimens using a group notation of letters indicating beam specifications with the following explanation: "Beam dimensions (width / height)" - "concrete type (HSC/RPC)" - "did not use steel fiber (NF) / use steel fiber (F)" - "did not use stirrup reinforcement (NS) / use stirrup reinforcement (S)".

Four pretension beam test specimens with 1:1 scale were made to investigate the behavior and performance of each beam. The first test specimen (beam #1) is a 30/50 HSC-70 MPa pretension beam, with stirrup reinforcement and concrete mix not using steel fiber (30/50-HSC-NF-S); the second test specimen (beam #2) is a 30/50 pretension RPC-120 MPa beam, with stirrup reinforcement and

concrete mix added steel fiber (30/50-RPC-F-S); the third test specimen (beam #3) is a 17/50 pretension RPC-120 MPa beam with stirrup reinforcement but the concrete mix does not added steel fiber (17/50-RPC-NF-S); The fourth test specimen (beam #4) is a 17/50 pretension RPC-120 MPa beam, not using stirrup reinforcement but added steel fiber (17/50-RPC-F-NS) as a concrete mixture.

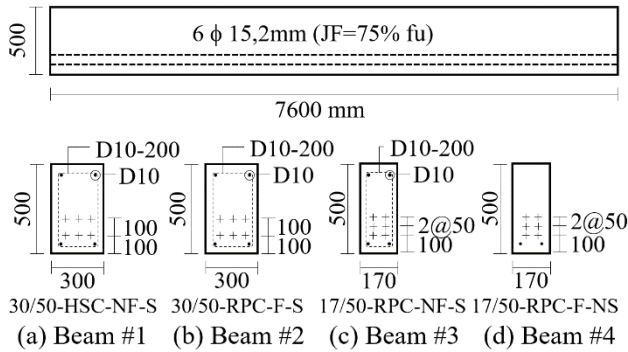


Figure 3 Beam Specimens Specification

The RPC mixture consists of nanometer-sized materials consisting of cement (1-100µm), silica fume (0.1-1µm), silica powder (0.1-100µm), silica sand (150–600 µm), water with low w/c ratio (below 0.28), superplasticizer admixture, and steel fiber. The composition of the concrete mixture for HSC and RPC used is shown in Table 1. The prestressing steel used was 15.2 mm dia strand with a breaking tensile strength of 1860 MPa and low-relaxation strand type. Longitudinal reinforcement and stirrups use was a diameter of 10 mm with a yield strength of 420 MPa. The specifications for prestressed steel and reinforcing steel are shown in Table 2. The specifications for Dramix 65/35BG steel fiber are shown in Table 3 and Figure 4.

Table 1 Concrete mixture of HCS and RPC

Material	Specification	Unit	HSC	RPC
Cement	OPC-1	kg/m3	630	950
Silica fume	92%	kg/m3	-	114
Silica Powder	max. 0.05mm	kg/m3	-	66
Silica sand	max. 0.6mm	kg/m3	-	1064
Natural sand	ex-Tayan	kg/m3	328	-
	ex-Cilegon	kg/m3	328	-
Coarse aggregate	ex-Cigudeg	kg/m3	998	-
Admixture	Tipe F	liter	10	27
Steel fiber	Dramix 65/35BG	kg/m3	-	160
Water		liter	130	209
	Sand / Cement	%	20	22
	Sand / Total Aggregate	%	40	100
	Steel fiber / Concrete Vol.	%	0	2

Table 2 Reinforcing material specifications

Steel	Dia. (mm)	Yield stress (MPa)	Tensile stress (MPa)	Modulus of Elasticity (GPa)
Rebar	10	Min.420	630	950
Strand	15.2	1674	-	114

Table 3 Steel fiber specifications (Dramix 35/65 BG)

Dia. d_f (mm)	Length L_f (mm)	Aspect Ratio (L_f/d_f)	Tensile stress (MPa)	Modulus of Elasticity (GPa)
0.55	35	65	1345	200

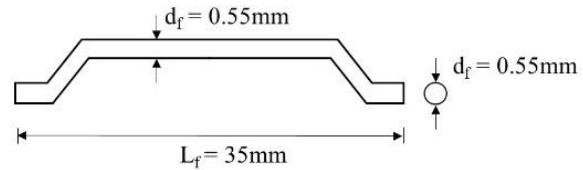


Figure 4 Size of steel fiber (Dramix 35/65BG)

Beam molds and concrete test sample molds are prepared on the factory beam production area. Prestressed steel (strand) is stretched along the beam production line. Both ends of the strand are moored to the anchor of the resistant block using a barrel-wedge which functions to lock to keep the tension on the prestressing steel working after the strand is withdrawn. One by one the strand is pulled by the mono jack until the stress on the strand reaches 1300 MPa or equivalent to 70% of the tensile stress (f_u). Figure 5 shows prestressed steel beams that have been stressed.

To investigate the mechanical properties of concrete, samples were made with variations of HSC, RPC with steel fiber and RPC without steel fiber. The type of concrete test, the dimensions of the test specimens and the number of test specimens made are shown in Table 4.



(a) Beam 17/50 Mold (b) Beam 30/50 Mold

Figure 5 Beam specimens mold

Table 4 Type of test and number of test specimens

Test Type	Dimensions (cm)	HSC (pcs)	RPC F (pcs)	RPC NF (pcs)
Compressive strength:				
1 day		3	3	3
4 day		3	3	3
7 day	Ø15/30	3	3	3
14 day		3	3	3
28 day		3	3	3
56 day		3	3	3
Modulus of elasticity	Ø15/30	2	2	2
UPV	Ø15/30	1	1	1
Split tensile	Ø15/30	3	3	3
Flexural tensile	15x15x60	3	3	3
Direct tensile	10x10x40	3	3	3

The beam specimens were made at the Wika Beton Factory in Bogor, West Java. Mixing in the batching plant uses a twin shaft mixer with a maximum mixing capacity of 2.2 m³. In the RPC manufacturing process, pre-weighed silica sand, silica powder and silica fume are put into the bucket hopper then brought up and poured into the mixer. In order for the mixer motor in the batching plant to mix easily or lightly, the RPC mix volume is set not to exceed 1.2 m³ or around 60% of the mixer capacity. Mixing with a larger volume can cause the mixer to not be able to rotate and can cause damage to the mixer motor. Mixing was carried out 4 (four) times in the following order: first mix 1.14 m³ for RPC beams 30/50-L7.6m, second mix 0.954 m³ for RPC beams 17/50-L7.6m and concrete test specimens, third mix 0.905 m³ for RPC beams without steel fiber 17/50-L7.6 m, and the fourth mix 1.356 m³ for HSC beams 30/50-L7.6 m and concrete test specimens. The volume of each mix is adjusted to produce 1 (one) beam and concrete test specimen in one mix. This is to avoid cold joints or anomalies caused by different stirring [9]. After the silica sand material, silica powder and silica fume enter the mixer, stirring is carried out in dry conditions for 5 minutes to mix the materials, and then cement is poured into the mixer and stirred again for 5 minutes. Furthermore, all the water and superplasticizer admixture are poured with a rotating blade mixer to mix the mixture. Stirring of the mixture was carried out until the mixture was evenly distributed and appeared to have good workability. The final stage of mixing is the addition of steel fiber to the mixture. Before the steel fiber is put into the mixer, the mix is taken and a flow table test is carried out to determine the flowability of the mix. Furthermore, the steel fiber is added gradually under the condition of the blade rotating until all of it is included in the mixture and the mixture is stirred for 2 minutes. The flow table test was again carried out to determine the flow properties of the mix after the addition of steel fiber. The process of pouring the RPC mixture into the mold of the beam test specimen and making the concrete test sample was carried out without using vibration. Mixed concrete in the mixer is poured into a cast bucket and then carried using a lift portal to the beam mold and the concrete is poured into the mold. From observations, the speed of the flow of the mixture in the mold flows slowly so that the pouring of the mixture is assisted by the movement of the cast bucket. The process of casting concrete is not assisted by a concrete compactor. After the mold is completely filled, trimming is carried out by leveling the top surface of the block. Furthermore, all test beam specimens and concrete test samples were covered with tarpaulin and left for 18 hours. Figure 6 shows the process of casting RPC beams.

The making of HSC beam test specimens with a compressive strength of 70 MPa follows the usual process carried out at PT Wika Beton. The result of mixing the HSC has good workability and the process of compacting the concrete uses an internal vibration device. The HSC beams and concrete test samples were then covered with tarpaulin to prevent water evaporation from the concrete. Curing concrete with hot steam (Steam Curing) begins after ± 18 hours after casting. Hot steam from the boiler is channeled into the tarpaulin covering the beam test specimen and the concrete sample until the temperature increases gradually to around 80 ± 5 °C. The temperature in the tarpaulin was

maintained for 66 hours without stopping, then the evaporation was stopped. Beams and concrete samples were naturally cooled for ± 8 hours. The steam curing process of the beam and concrete specimens are shown in Figure 7.



Figure 6 The process of making RPC Beam



Figure 7 Treatment of concrete with high temperature steam (steam curing)

The compressive strength test was carried out on 3 (three) concrete cylinders to ensure that the compressive strength of the concrete was sufficient to transfer the prestressing force from the strands. The beam molds are disassembled and strand is detensioned then cut. Concrete test samples are stored in dry conditions without wet treatment according to the same treatment conditions on the beam. Several concrete test samples have been tested before and after steam curing to obtain information on concrete at an early age and periodic testing is carried out until the concrete is 28 days.

D. TESTING OF TEST SPECIMENTS

Preparation of test specimens and concrete testing procedures are carried out in accordance with the Indonesian National Standard (SNI), other international standards and references from previous research journals. The test procedure as a reference for testing the mechanical properties of concrete is shown in Table 5. For compressive strength test of RPC concrete, prior to the steam curing treatment process, all concrete cylinder specimens were removed from the mold at +/- 16 hours of age, then the top surface of the cylinder was leveled using a grinding tool. This is done so that the grinding process is easier to do because the compressive strength of RPC concrete is still not too high. Figure 8 shows the process of leveling the surface of a concrete cylinder by grinding. As for the HSC concrete cylinder sample, leveling of the cylinder surface using high strength gypsum was carried out just before the compressive strength test.

Table 5 Concrete test and references

Type of Test	References
Compressive strength	SNI 03-1974-2011
Modulus of elasticity	SNI 03-4169-1996
Splitting tensile test	SNI 03-2491-2002
Flexural tensile test	SNI 03-4154-1996
Direct tensile test	Yudhanto et al.[13]
Test UPV	SNI ASTM C597-2012



Figure 8 Surface preparation of cylinder specimen with grinding tool

The beam static load test was carried out at the Research Laboratory of PT Wika Beton. Prior to testing, an inspection of the beam test specimen is carried out to ensure that there are no defects in the beam. Visual inspection of beams #1, #2 and #4 did not reveal any defects, however, cracks were found on beam #3 on the upper surface of the beam. Cracks are clearly visible at 5 (five) different points in a direction parallel to the width of the beam. Beam #3 (17/50-RPC-NF-S) uses RPC mixture which does not use steel fiber. All cracks were investigated by measuring the width and depth of the crack using a UPV tool and then repaired using high quality repair materials. The results of the repair are checked again with the UPV tool to ensure that the crack has been filled and covered with repair material. Examination of cracks on the surface of beam #3 is shown in Figure 9.



Figure 9 Crack depth testing with UPV tool

The bending test of beams with static loads is carried out using the 4 (four) loading point method. The beam is placed on two pedestals with the roller axle distance of 300mm from the end of the beam. The steel beam functions is to transfer the compressive load from the piston cylinder jack is placed at the top of the beam. The transfer beam rests on 2 (two) roller supports with symmetrical support rollers positioned at a distance of 1m from the center of the beam. The compressive load is obtained from a cylinder jack mounted on a bending test frame and connected to an electric hydraulic pump. The load cell is installed between the piston cylinder and the transfer beam to read the compressive load. A total of 5 (five) Linear Variable

Differential Transformer (LVDT) sensors were installed at locations 1.2 m, 2.5 m, 3.5 m, 4.5 m and 5.8 m from the axle of the left side beam support roller. LVDT serves to measure the deformation and curvature profile of the beam when loading. The load cell and LVDT are connected to a data logger device which records the history of loads and deformations occurring at the same time. Schematic of the static load bending test is shown in Figure 10 and the position of the beam for the bending test is shown in Figure 11.

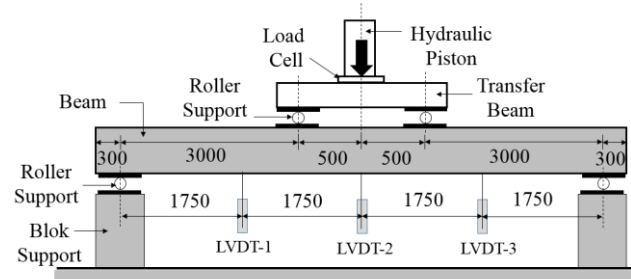


Figure 10 Schematic of beam static load test



Figure 11 Beam static vertical load test

Vertical compressive loads act on the beam gradually and the beam is observed to find the first visible cracks on the surface of the beam. After the initial crack was found, the observation was continued to find cracks up to 0.3 mm wide. Furthermore, the vertical load continues to be increased until the beam can no longer provide resistance to vertical loads. The vertical load and deformation recording data obtained are then processed to investigate beam behavior.

RESULTS AND DISCUSSIONS

A. MIXTURE FLOWABILITY

The results of the RPC mix flow test using the flow table test equipment are shown in Figure 12. The average diameter size of the mix distribution before the addition of steel fiber was > 250 mm. After steel fiber added to the mix, the average diameter of the flow table test distribution was reduced to 230 mm. Referring to journal [14], the nature of the RPC mixture is classified as a fluid mixture. Visually, the RPC mix is homogeneous, does not experience segregation and has good cohesion. The RPC mix flows smoothly when it is poured from the mixer into the cast mobile bucket. Furthermore, the same thing happened during the process of pouring the mixture into the mould. A small amount of steel fiber appeared to be obstructed and collected at the outlet of the cast mobile

bucket, but did not impede the outflow of the slurry. The flow properties of the RPC mix during the manufacture of the test specimens decreased significantly, within +/- 10 minutes, the mixture that had been poured from the mobile bucket cast into the container for the making of concrete specimens appeared to be no longer flowing. This is due to the use of large amounts of silica which causes rapid hardening of the concrete surface. This condition can lead to the formation of cold joints in concrete when the pouring process is not carried out simultaneously and it is difficult to smooth the surface of the concrete [15]. The surface of the thin top layer of the beam has hardened not too long after casting. Meanwhile, steel fiber does not appear on the surface of the beam.

For HSC the flowability of the mix is investigated by slump flow test. The average diameter of the concrete spread is 650 mm. The concrete mix looks homogeneous and no segregation occurs. During the process of making concrete samples, the mix still has good workability making it easier to make test specimens.



Figure 12 Flow table test and visual of concrete flow

B. COMPRESSION STRENGTH

The results of the compressive test of concrete cylinder specimens are shown in Table 6 and the graph of compressive strength against the age of concrete is shown in Figure 13. The compressive strength of HSC, RPC with fiber (RPC-F), and RPC without steel fiber (RPC-NF) at age 1 (one) day or before the steam curing process is 47,49 MPa, 54,48 MPa and 60,21 MPa respectively. After the steam curing process was completed, the compressive strength of concrete at 4 days old increased significantly to 62,09 MPa, 91,68 MPa and 95,59 MPa.

Table 6 Average concrete compressive strength

Concrete Age	Average Compressive Strength (MPa)		
	HSC	RPC-F	RPC-NF
1 day (before steam curing)	47,49 (SD 1.5)	47,49 (SD 1.5)	60,21 (SD 1.9)
4 day (after steam curing)	62,09 (SD 6.1)	91,68 (SD 2.5)	98,59 (SD 4.1)
7 day	71,82 (SD 0.8)	100,24 (SD 2.3)	109,68 (SD 2.5)
14 day	75,32 (SD 2)	106,94 (SD 3.0)	115,24 (SD 2.9)
28 day	78,10 (SD 1.1)	111,07 (SD 0.9)	125,10 (SD 3.6)

This value already meets the minimum compressive strength of concrete on beams to withstand the transfer of

prestress forces, namely 35 MPa for HSC concrete and 75 MPa for RPC concrete. The average compressive strength continues to increase until the age of the concrete is 28 days where the compressive strength of the concrete achieved is 78,1 MPa, 108,88 MPa and 123,27 MPa respectively.

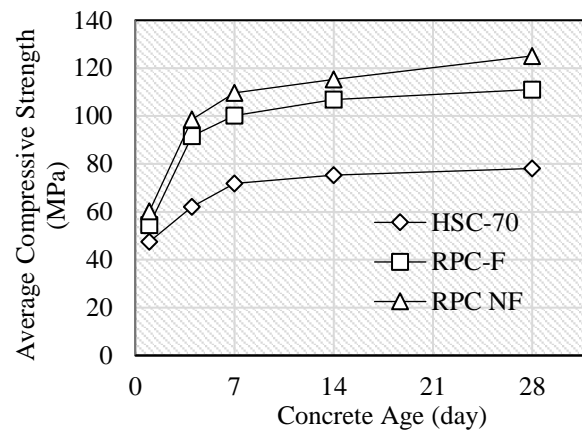


Figure 13 Graph of average compressive strength against concrete age HSC-70, RPC-F and RPC-NF

A significant increase in compressive strength occurred after the steam curing process on the RPC-F specimens of 68% and 63% of RPC-NF. Whereas in HSC concrete the increase was only 30% to the compressive strength of concrete aged 1 day (before the steam curing process). This was also found in the research conducted by Park where the concerned stated that curing concrete using hot steam at high temperatures can ensure an increase in the compressive strength of concrete [8]. The compressive strength of RPC-F concrete is always lower than RPC-NF concrete for all ages of testing. For 28 days of concrete, RPC-NF concrete has a 12% higher compressive strength compared to RPC-F concrete. This result is different from the research that was done by Abdelrahim [16] where the addition of steel fiber resulted in an increase in the compressive strength of concrete. This difference may be due to the uneven distribution of steel fiber in the specimen. From the observation of the specimens failure, the HSC and RPC-NF experienced explosive destruction and concrete fragmentation occurred. Unlike the case with the RPC-F, the failure was not sudden. The failure of three different material specimens is shown in Figure 14.



(a) HSC-70MPa (b) RPC-F (c) RPC-NF

Figure 14 Failure of concrete test specimens cylinder HSC-70, RPC-F and RPC-NF

C. MODULUS OF ELASTICITY

The elastic modulus of concrete at 4 and 28 days of age are shown in Table 7 and Figure 15. The elastic modulus of each material were obtained from 1 (one) test of the specimen. The order from the lowest value to the highest value at the age of 28 days were HSC, RPC-F and RPC-NF with values of 33,1 GPa, 43,5 GPa and 44,7 GPa. The values of the modulus of elasticity do not show a significant difference to the modulus of elasticity of the concrete aged 4 days (after the steam curing).

Table 7 Modulus elasticity of concrete

Concrete Age (days)	Modulus Elasticity (GPa)		
	HSC-70	RPC-F	RPC-NF
4	32,8	42,5	44,9
28	33,7	42,7	44,7

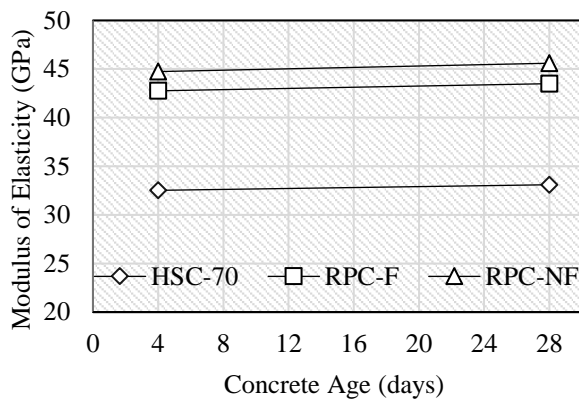


Figure 15 Graph of concrete elasticity modulus value against concrete age HSC-70, RPC-F and RPC-NF

D. TENSILE STRENGTH

The tensile strength values of concrete at 28 days are shown in Table 8 and Figure 16. The RPC-F sample produced the highest tensile strength, followed by RPC-NF and the lowest was HSC. The use of steel fiber as much as 2% of the concrete volume in RPC-F concrete, resulted in a tensile strength for direct tensile, split tensile and flexural tensile tests 30%, 55% and 88% higher than RPC-NF. This shows that the use of steel fiber is very effective in increasing the tensile strength of concrete.

Table 8 Average tensile strength value of concrete

Tensile Test Type	Average Tensile Strength (MPa)		
	HSC-70	RPC-F	RPC-NF
Direct Tensile	4,2 (SD 0.22)	6,16 (SD 0.28)	4,75 (SD 0.37)
Split Tensile	4,62 (SD 0.61)	8,26 (SD 0.46)	5,34 (SD 0.46)
Flexural Tensile	5,10 (SD 0.11)	14,63 (SD 0.05)	7,78 (SD 0.05)

E. ULTRASONIC WAVE VELOCITY

The results of ultrasonic wave velocity readings on cylinder test samples using the UPV test equipment are shown in Table 9 and Figure 17. The speeds of UPV wave for HSC, RPC-F and RPC-NF before steam curing were 4248 m/s,

4266 m/s and 4309 m/s sequentially. The speed of wave after the steam curing (age 4 days) results in an increase in speed to 4601m/s, 4631m/s and 4680m/s respectively. However, in subsequent tests, when the concrete samples were aged 14 days and 28 days, the wave velocity values did not differ much from the values at the 4-day age test. The results above show that the steam curing is effective in accelerating the hydration process in concrete as indicated by the increase in UPV wave velocity. The RPC-F wave speed value is lower than RPC-NF for each age of the test specimens. This result correlates with the concrete compressive strength test value. From the results of the wave velocity, all concrete samples are classified as very good concrete according to ASTM C597-2012 [17].

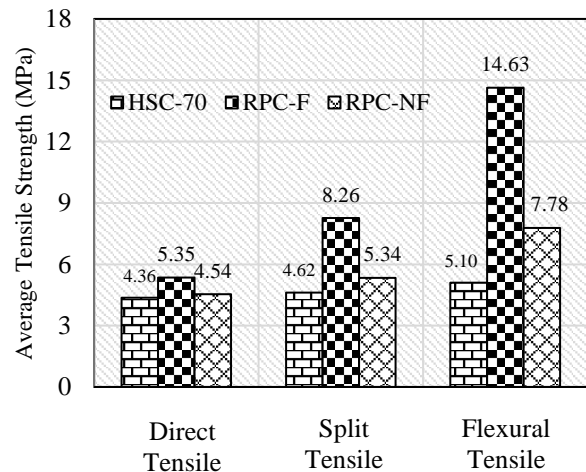


Figure 16 Graph of average tensile strength value of concrete at 28 days of age for HSC-70, RPC-F and RPC-NF concrete for 3 (three) different types of tensile tests.

Table 9 Average ultrasonic wave velocity

Concrete Age	Average Wave Velocity (mm/s)		
	HSC	RPC-F	RPC-NF
1 day (before steam curing)	4248 (SD 4.9)	4266 (SD 10.2)	4309 (SD 20.8)
4 days (after steam curing)	4601 (SD 14.7)	4631 (SD 7.1)	4680 (SD 16.6)
14 days	4614 (SD 9.9)	4643 (SD 24.7)	4665 (SD 41)
28 days	4597 (SD 3.3)	4658 (SD 7.1)	4673 (SD 7.5)

F. VERTICAL LOAD AND DEFLECTION

The vertical load and deflection at the time of the initial cracking and failure of the beam are shown in Table 10, while in graphical form the relationship between the vertical load and the beam deflection is shown in Figure 18.

Table 10 Maximum load and deflection of the beam

Remark	Unit	30/50	30/50	17/50	17/50
		HSC-NF-S	RPC-F-S	RPC-NF-S	RPC-F-NS
Load	kN	421	457	295	387
Deflection	mm	145	164	121	118

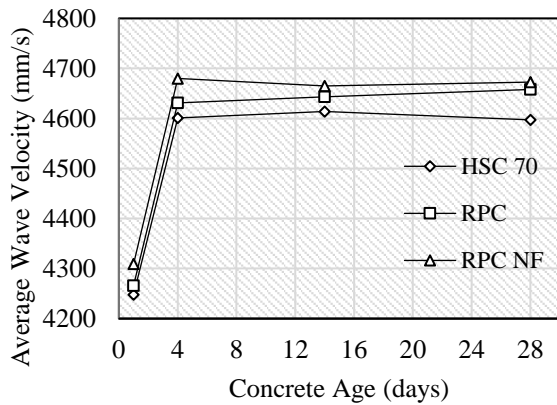


Figure 17 Graph of UPV tool wave velocity value against concrete age for HSC-70, RPC-F and RPC-NF

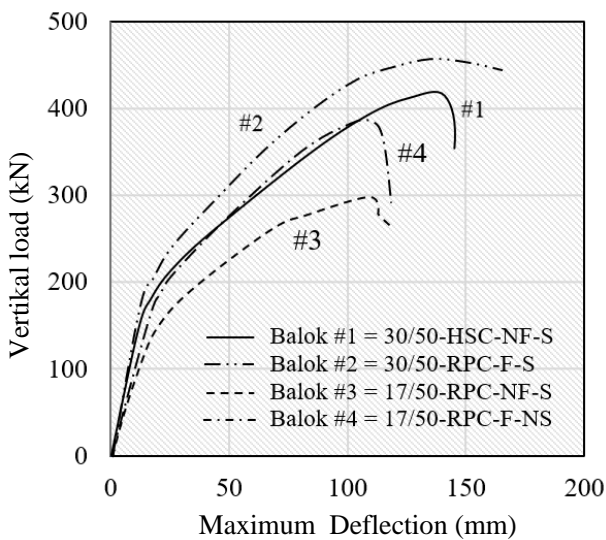


Figure 18 Graphs of vertical load against deflection at midspan for test beams #1, #2, #3 and #4.

In the initial loading conditions, the deflection that occurs shows that the beam is still in an elastic condition. For beams using steel fiber in a concrete, a higher load can maintain a longer elastic condition than beams with the same dimensions but not using steel fiber. In the inelastic condition, the curve of beam #1 is visible adjacent to beam #4. This shows that even though beam #4 has slimmer dimensions, the stiffness value is almost the same as beam #1. While beam #3 which has the same dimensions as beam #4 has the lowest stiffness. Beam #2 shows the highest stiffness value. From the above it can be concluded that steel fiber material results in an increase in beam stiffness. Steel fiber maintains the cross-sectional shape of the beam is maintained along with the increase in load so that the beam does not experience brittle destruction.

G. MOMENT-CURVATURE

The relationship of the moment to the curvature of the beam is shown in Figure 19. The graph shows the deformability (ductility) for each beam. The ability to deform can be seen from the large area under the bending moment curve. It can be seen that beam #2 has the greatest

ductility, then beam #1, beam #4 and beam #3. Ductility Beam #4 and beam #1 show almost the same ductility. This correlates with the stiffness value of the beam. Steel fiber not only results in an increase in the stiffness of the beam but plays a role in increasing the deformability of the beam.

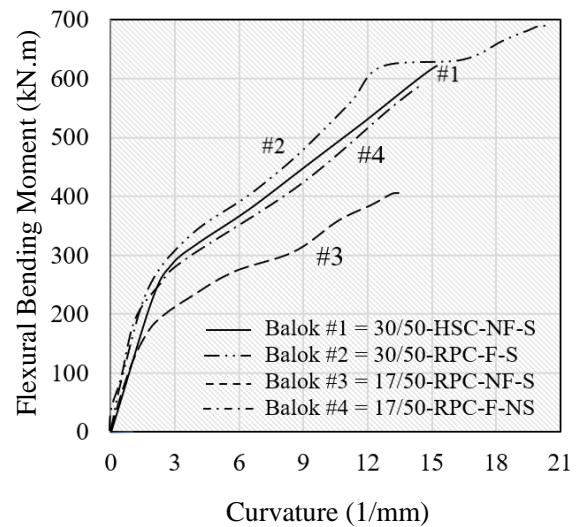


Figure 19 Graph of the flexural bending moment of the beam against the curvature of the specimen beam #1, #2, #3 and #4.

H. FAILURE MODE OF BEAM SPECIMENTS

The failure mode of the beam test specimens at the maximum vertical load is shown in Figure 20. All beams show an initial crack at the bottom of the beam occurring at several locations between transfer beam placements. The propagation of these cracks continues to increase with increasing vertical compressive loads. The beam failure process that occurs shows different failure behavior between beams using steel fiber and beams that do not use steel fiber.

For beam #2 (300/500-RPC-F-S) and beam #4 (170/500-RPC-F-NS) the beam failure process does not show fragmentation towards peak load. In beam #2, the crack that occurs at the bottom of the beam at the right side transfer beam support location continues to crack with increasing load and resulting deflection. Prestressed steel breaks marked with a thump and from the load cell sensor it shows that the vertical load has suddenly dropped. On beam #4 the peak load is indicated by damage to the upper surface of the beam just below the support of the left side transfer beam. During the peak vertical load the damage occurs on the top surface and at the same time cracks appear in the beam web in a horizontal direction. The horizontal direction cracks that occur are caused by the beam dimensions that are too slender. There is no indication of the prestressing steel breaking at maximum load. The condition of the damaged concrete does not show fragmentation or pieces of concrete that are detached from the beam. For beams without steel fiber, namely beam #1 (300/500-HSC-NF-S) and beam #3 (170/500-RPC-F-NS) indicate brittle concrete. The failure of the beam occurs suddenly and the concrete fragments at the damage failure. On beam #1, the top surface of the beam at the support of the transfer beam on the right side begins to suffer damage when it approaches the peak vertical load. During the peak

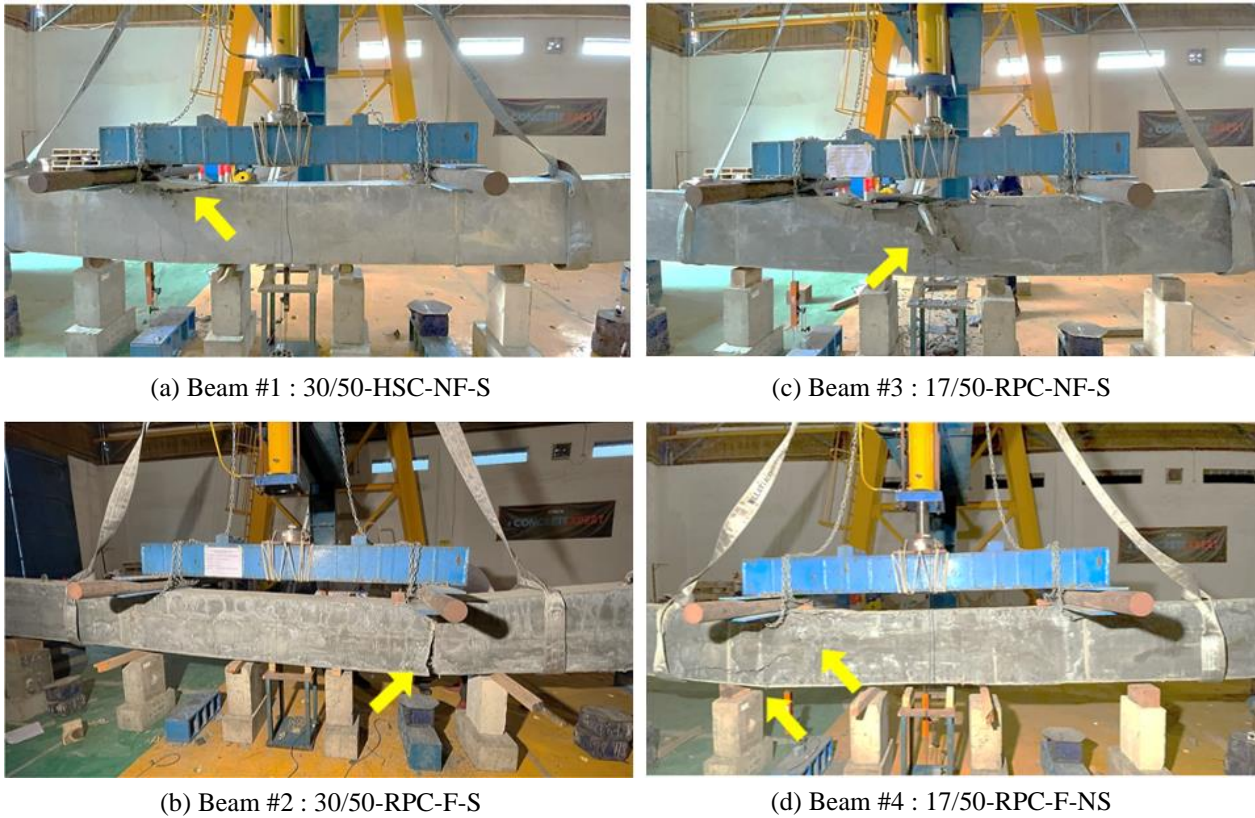


Figure 20 Failure mode of beam under maximum vertical load static load test for beam #1, beam #2, beam #3 and beam #4.

load the concrete suddenly collapses and causes chunks of concrete on the top surface of the beam. Meanwhile, beam #3 on the upper surface between the supports of the transfer beams begins to show cracks and peels off in the form of thin slabs about 1–2 cm thick which increases with increasing vertical loads. When the peak load on the top surface and both sides of the beam in the middle section crumbles suddenly causing large chunks of slab to be detached from the beam. There were no signs of broken prestressing steel at maximum loading.

From the failure mode of the beams, it shows the same results as previous studies by Chen [18] where in the conclusion of the research report stated that steel fiber effectively prevents brittle destruction and maintains its initial shape after reaching the peak vertical load with not large deformation. The same thing was also reported by Branch and Kim's research [10] which stated that steel fiber made a good ductility response compared to concrete without steel fiber which immediately crumbled when it reached its peak load. In addition, this is in line with research conducted by Ngo and Kim [3] who concluded that steel fiber provides a bridging effect on concrete so that the failure mode is ductile and the material does not experience fragmentation.

I. FLEXURAL STRENGTH COMPARED TO THE THEORITICAL VALUE

The reserve strength of the beam test specimens after experiencing cracking is shown in Table 11. The nominal moment used is equal to the moment of bending resistance at fracture multiplied by the reduction factor. Of the four

beam specimens, all beam specimens met the requirements for a beam capacity ratio of greater than 1.2.

Table 11 Ratio of beam flexural strength after cracking

Remarks	30/50 HSC- NF-S	30/50 RPC- F-S	17/50 RPC- NF-S	17/50 RPC- F-NS
Cracking Moment (M_{cr})	226	245	247	242
Breaking Moment (M_{br})	632	687	444	581
ϕ	0.9	0.9	0.9	0.9
$\phi M_{br}/M_{cr} > 1.2$	2.52	2.53	1.61	2.16

The theoretical moment of resistance calculation of the four beams is shown in Table 12, loss of prestressing force calculation is shown in Table 13 and the calculation of the reserve strength of the beam after experiencing cracking is shown in Table 14. The theoretical calculation analysis uses the average concrete compressive strength value and the elastic modulus value of the concrete cylinder test sample 28 days. Comparison of the flexural strength results of the static load test of the beam against theoretical calculations is shown in Table 15. The fracture moment values of the four beams tested were greater than the theoretical calculations with the ratio of beam #1, beam #2, beam #3 and beam #4 of 1.22, 1.22, 1.45 and 1.43 respectively. While the maximum flexural strength values of only beam #1, beam #2 and beam #4 are greater than theoretical calculations with ratios of 1.33, 1.37 and 1.30

Table 12 Bending resistance of the beam (theoretical)

Notation	Unit	30/50 HSC-NF-S	30/50 RPC-F-S	17/50 RPC-NF-S	17/50 RPC-F-NS
f'_c	MPa	78,1	111,07	125,1	111,07
B	mm	300	300	170	170
D_p	mm	350	350	350	350
D	mm	455	455	455	455
d'	mm	45	45	45	45
A_{ps}	mm ²	840	840	840	840
		6φ15.2	6φ15.2	6φ15.2	6φ15.2
A_s	mm ²	157	157	157	-
		2D10	2D10	2D10	-
A_s'	mm ²	157	157	157	-
		2D10	2D10	2D10	-
f_{ps}	MPa	1724	1724	1724	1724
f_y	MPa	420	420	420	420
f_s'	MPa	360,2	262,5	381,8	405,5
$Wp + (w-w')\frac{d}{a_p}$		0.103	0.115	0.103	0.073
$0.36 \beta 1$		0.234	0,234	0,234	0,234
A	52,0	80,4	90,2	83.51	83.51
M_n	497	476	441	446	446
ϕM_n	447	428	397	402	402

Table 13 Loss of prestress loss (theoretical)

Notation	Unit	30/50 HSC-NF-S	30/50 RPC-F-S	17/50 RPC-NF-S	17/50 RPC-F-NS
f_{pu}	MPa	1860	1860	1860	1860
JF	%	70	70	70	70
f_{pi}	MPa	1302	1302	1302	1302
A_{ps}	mm ²	840	840	840	840
		6φ15.2	6φ15.2	6φ15.2	6φ15.2
P_i	kN	1094	1094	1094	1094
e	mm	100	100	100	100
A_c	mm ²	150E3	150E3	85E3	85E3
I_c	mm ⁴	1,5E12	1,5E12	8,8E11	8,8E11
M_D	Nmm	21622	21622	12253	12253
f_{cs}	MPa	7,30	7,30	12,88	12,88
E_{ps}	GPa	200	200	200	200
E_{ci}	MPa	32500	42800	44700	42800
E_c	MPa	33100	43500	45600	43500
t	hari	1825	1825	1825	1825
Δf_{PES}	MPa	44,9	34,1	57,6	60,2
Δf_{PR}	MPa	21,5	21,5	21,5	21,5
Δf_{PCR}	MPa	93,3	71,0	119,5	1,3
	MPa	159,2	159,2	159,2	159,2
Δf_{PT}	MPa	318,9	285,8	357,9	366,2

Table 14 Reserves of flexural strength after cracking

Notation	Unit	30/50 HSC-NF-S	30/50 RPC-F-S	17/50 RPC-NF-S	17/50 RPC-F-NS
f_{pu}	MPa	1860	1860	1860	1860
Δf_{PT}	MPa	318,9	285,8	357,9	366,2
f_{pe}	MPa	983,1	1016,2	944,1	935,8
A_{ps}	mm ²	840,0	840,0	840,0	840,0
P_{eff}	kN	825,8	853,6	793,1	786,1
S_c	mm ³	1,25E+7	1,25E+7	7,08E+6	7,08E+6
f_r	MPa	2,92	3,48	3,69	3,48
M_{crk}	kN.m	188	200	172	169
$\phi M_n / M_{cr}$		2.30	2,30	2,24	2,50

respectively. In beam #3, the ratio of the tested flexural strength to the theoretical flexural strength is 0.94.

CONCLUSIONS

This experiment studied the use of Reactive Powder Concrete (RPC) materials which are made using local

materials available in Indonesia for pre-stressed beams in highway bridge structures. Physical and mechanical properties such as mix flowability, compressive strength, elastic modulus, tensile strength properties, and concrete density were observed for HSC-70 MPa, RPC-120 MPa and RPC-120 MPa without steel fiber. To study the

physical and mechanical properties of all materials, concrete test samples were made for various materials and 4 (four) prestressed pre-tensioned beams were made with a scale of 1:1 to study the strength and response of the beam from the loading test until the beam experienced failure.

Table 15 Comparison of bending strength values of static load test results against theoretical

Remarks	Flexural Strength of Beam (kN.m)			
	30/50 HSC- NF-S	30/50 RPC-F- S	17/50 RPC- NF-S	17/50 RPC- F-NS
First Cracks				
1. Experiment	226	245	247	242
2. Theoretical	188	200	172	169
Experiment/ Theoretical	1.22	1.22	1.45	1.43
Beam breaks				
1. Experiment	632	687	444	581
2. Theoretical	481	497	476	441
Experiment/ Theoretical	1.33	1.37	0.94	1.30

Some of the main things found in this test are as follows:

1. A mixture of Reactive Powder Concrete (RPC) made on a production scale for the making beams test specimens shown a mixture easily flows into the mold without the aid of a vibrator. The flowing nature of the mix did not last long because in about +/- 10 minutes the top surface had hardened. This is due to the use of silica material in large quantities which causes rapid hardening of the concrete surface.
2. Concrete treatment with hot steam (steam curing) at $80 \pm 5^\circ\text{C}$ for 66 hours, is effective for accelerating the development of the compressive strength of RPC. This is indicated by the increase in compressive strength of the concrete samples before and after the steam curing process.
3. The cylinder compressive strength value of 10/20 for RPC concrete using steel fiber was obtained 111 MPa lower than the compressive strength of RPC which did not use steel fiber which reached 125 MPa. The difference in these results is the possibility that the distribution of steel fiber on the compressive strength test specimens is uneven because the size of the cylindrical test object used is too small, or due to the steel fiber's own weight which causes it to tend to sink to the bottom of the cylinder
4. The quality of HSC and RPC is classified as very good based on the wave velocity value of the UPV tool. This shows that the casting of RPC concrete without compaction result a dense concrete.
5. From the comparison between the test results and the theoretical value, it was found that all the beams tested result a higher breaking moment value than the theoretical value, while the breaking moment value contained 1 (one) beam, namely beam #3 (170/500-RPC-NF-S) which the value of the breaking moment is lower than the theoretical value.
6. The failure mode of the beam shows that the beam using steel fiber does not collapse suddenly while the failure mode of the beam without steel fiber occurs suddenly,

explosively accompanied by fragmentation of the concrete from the beam.

7. The use of steel fiber with the specifications used is able to prevent shrinkage cracking in the beam, increase the tensile strength of the concrete, maintain the integrity of the beam, prevent explosive concrete destruction, prevent concrete fragmentation during peak loads so that the beam can expand maximum flexural strength and produces greater stiffness and better deformability (ductility) than beams without steel fiber.
8. RPC made with local natural materials produces concrete with very high performance. This is shown from the results of the mechanical properties test of RPC concrete which is higher than HSC concrete.
9. RPC concrete that uses steel fiber can meet the design requirements for flexural strength of beams according to SNI 1725-2016 code and implementation on an industrial scale has been able to be carried out by PT Wika Beton as a precast concrete producer.

Suggestions for further research topics are in addition to formulating the modulus of elasticity with more test samples, also research that can make the cost of making RPC concrete more efficient as well as research to find the most efficient and optimal steel fiber content in the RPC composition, research on the use of alternative types of fiber used in concrete mixes and research to find efficient and optimal steam curing time and temperature.

REFERENCES

- [1] M. K. Tadros, A. Sevenker, and R. Berry, "Ultra-high-performance concrete a game changer", *PCI Journal*, vol. 65, no. 3, pp. 33-36, 2019.
- [2] T. Zych, "New Generation Cementitious Composites With Fibres", *Technical Journal*, vol. 15, pp. 85-102, 2014.
- [3] T. T. Ngo and D. J. Kim, "Synergy in shear response of ultra-high-performance hybrid-fiber-reinforced concrete at high strain rates", *Composite Structures*, vol. 195, pp. 276-287, 2018.
- [4] S. A. Nurjannah, B. Budiono, and I. Imran, "Non-linear numerical modelling of partially pre-stressed beam-column sub-assemblages made of reactive powder concrete", *Journal of Engineering and Technological Sciences*, vol. 51, pp. 28-47, January 2019. (references)
- [5] H. Hardjasaputra, V. Indrawati, and I. Djohari, "Pengaruh penggunaan serat polypropylene dan micro steel fiber pada ketahanan api dari ultra high performance concrete (UHPC) untuk bangunan infrastruktur", *Konferensi Nasional Teknik Sipil 7 (KoNTekS 7)*, pp. 17-23, 2013.
- [6] A. Sugathan, "Steel reinforced reactive powder concrete", *International Journal of Advanced Engineering Research and Science*, vol. 3, pp. 150-157, 2016.
- [7] S. A. Nurjannah, B. Budiono, and I. Imran, "Potensi Reactive Powder Concrete Sebagai Material Elemen Struktur", *Teras Jurnal*, vol 3, no 2, pp. 157-166, 2013.

- [8] J. S. Park, Y. J. Kim, J. R. Cho, and S. J. Jeon, "Early-age strength of ultra-high performance concrete in various curing conditions", *Materials (Basel)*, vol. 8, no. 8, pp. 5537-5553, 2015.
- [9] J. P. Binard, "UHPC: A game-changing material for PCI bridge producers", *PCI Journal*, 2017.
- [10] I. Branch and Y. J. Kim, "Development of cost-effective ultra-high performance concrete (UHPC) for Colorado's sustainable", *Colorado Department of Transportation*, Report No. CDOT-2018-15, 2018.
- [11] B. S. Nasional, *Pembebanan untuk Jembatan (SNI 1725: 2016)* (Jakarta: Standar Nasional Indonesia). 2015 (Draft).
- [12] B. S. Nasional, *Perencanaan struktur beton untuk jembatan (RSNI T-12-2004)* (Jakarta: Standar Nasional Indonesia). 2014 (Draft).
- [13] F. A. Yudhanto, A. S. Budi, and H. A. Saifullah, "Kajian uji tarik beton HVFA memadat sendiri terhadap beton normal", *Matriks Teknik Sipil*, vol. 7, no. 4, 2019.
- [14] N. P. C. Association, "Ultra high performance concrete (UHPC) - guide to manufacturing architectural precast elements," *NPCA White Paper*, 2013.
- [15] EFNARC, *The european guidelines for self-compacting concrete*, May, 2005.
- [16] M. A. A. Abdelrahim, A. Elthakeb, U. Mohamed, and M. T. Noaman, "Effect of steel fibers and temperature on the mechanical properties of reactive powder concrete", *Civil and Environmental Engineering*, vol. 17, no. 1, pp. 270-276, 2021.
- [17] B. S. Nasional, *Metode uji kecepatan rambat gelombang melalui beton (ASTM C597:2012)* (Jakarta: Standar Nasional Indonesia). 2012 (Draft).
- [18] H. J. Chen, Y. L. Yu, and C. W. Tang, "Mechanical properties of ultra-high performance concrete before and after exposure to high temperatures", *Materials*, vol. 13, no. 3, pp. 1-17, 2020.